NASA TECHNICAL NOTE

NASA TN D-3784

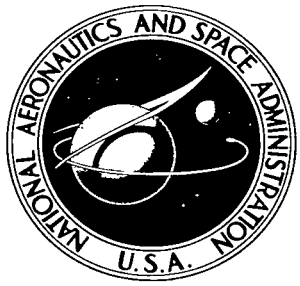

C. 1

TECH LIBRARY KAFB, NM
0130516

LOAN COPY: RETURN TO
AFWL (WLIL-2)
KIRTLAND AFB, N MEX

NASA TN D-3784

ANALOG-COMPUTER STUDY OF PARASITIC-LOAD SPEED CONTROL FOR SOLAR-BRAYTON SYSTEM TURBOALTERNATOR

by Roy C. Tew, Robert D. Gerchman, and Herbert G. Hurrell

Lewis Research Center
Cleveland, Ohio

NATIONAL AERONAUTICS AND SPACE ADMINISTRATION • WASHINGTON, D. C. • JANUARY 1967

TECH LIBRARY KAFB, NM
0130516

NASA TN D-3784

ANALOG-COMPUTER STUDY OF PARASITIC-LOAD SPEED CONTROL FOR SOLAR-BRAYTON SYSTEM TURBOALTERNATOR

By Roy C. Tew, Robert D. Gerchman, and Herbert G. Hurrell

Lewis Research Center
Cleveland, Ohio

NATIONAL AERONAUTICS AND SPACE ADMINISTRATION

For sale by the Clearinghouse for Federal Scientific and Technical Information
Springfield, Virginia 22151 – Price $2.00

ANALOG-COMPUTER STUDY OF PARASITIC-LOAD SPEED CONTROL FOR SOLAR-BRAYTON SYSTEM TURBOALTERNATOR

by Roy C. Tew, Robert D. Gerchman, and Herbert G. Hurrell

Lewis Research Center

SUMMARY

An analog-computer study was made of a parasitic-load speed control. The control studied is of the type being designed for a 10-kilowatt turboalternator of a Brayton-cycle space power system. The steady-state performance, transient response, and stability of the control system were investigated. Transients were introduced by stepping the alternator vehicle load off, allowing the system to reach steady state, and then stepping the vehicle load on. Ranges of controller parasitic-load capacity, overall gain, and time constants were studied.

The simulated control with design time constants satisfied both the steady-state and the transient specifications with parasitic-load capacities equal to or greater than 10 kilowatts for the particular transients studied. A capacity greater than 10 kilowatts, however, should be used to provide positive control. For 12- and 18-kilowatt capacities, the controller time constants can be several times their design values before speed response fails to meet specifications. For the 12- and 18-kilowatt capacities, the time constants were increased until step removal of the vehicle load resulted in a sustained oscillation of the speed. Instability also occurred for design time constants but with the controller gain between 10 and 20 times the design value.

Studies showed that the speed control oscillates in response to an unstable voltage regulator, but the amplitude of speed oscillations is very small.

INTRODUCTION

There is considerable interest in the potential of space power systems that employ the Brayton thermodynamic cycle. One such system, a solar-Brayton system, is currently being studied at the Lewis Research Center. The power into the system is solar energy collected by a parabolic mirror, stored in an absorber, and then transferred to

the argon working gas. The hot argon gas imparts its energy to two turbines. The first turbine drives the compressor, and the second drives the alternator, which produces 10 kilowatts of electrical output power. The closed Brayton loop is completed with a recuperator and a heat exchanger that rejects heat to a liquid radiator loop.

Certain alternator loads in space power applications operate only in a narrow frequency range. Since alternator electrical frequency is directly related to turboalternator speed by the number of alternator poles, the speed must be controlled within a narrow range.

There are two general methods of controlling turbine speed: One method is to control the turbine torque by regulating the fluid power into the turbine. Such a method, using valves to allow for a bypass of the fluid around the turbine, has been studied for the solar-Brayton turboalternator (ref. 1). The other method is to control the load torque by use of a parasitic load in conjunction with the vehicle load.

The speed control being designed for the solar-Brayton turboalternator is of the parasitic electrical load type in which the control senses alternator frequency. If the vehicle load is switched off, the speed increases and, hence, frequency goes above the set point. The control reacts by gating current into the parasitic load. An increase in power dissipation results and creates an increase in the load torque that balances the turbine torque. Acceleration is thus reduced to zero. Since the speed control has no reset action, the steady-state frequency is maintained above the set point for this condition of no vehicle load. When the vehicle load is switched on, the speed decreases, and the control decreases the amount of current flowing into the parasitic load. The load torque thus decreases to balance the turbine torque, and the turbine speed settles out at the system design point.

In order to evaluate the design of this control in relation to the required performance specifications, the speed control and the turboalternator (with its voltage regulator) were simulated on an analog computer. A study was made of the control performance when the system was subjected to 10-kilowatt vehicle-load transients. Since the gain and time constants of a fabricated control may not duplicate the design values, the study was made for ranges of gain and time constants. A range of parasitic-load capacities was also studied. From the studies, the steady-state speed error, transient response, and stability characteristics were determined and are discussed herein. Also discussed are interactions of the speed control and the voltage regulator. The report includes a brief description of the speed control design and the computer simulation.

DESCRIPTION OF CONTROL AND COMPUTER SIMULATION

The performance of the control was evaluated with respect to the following specifications:

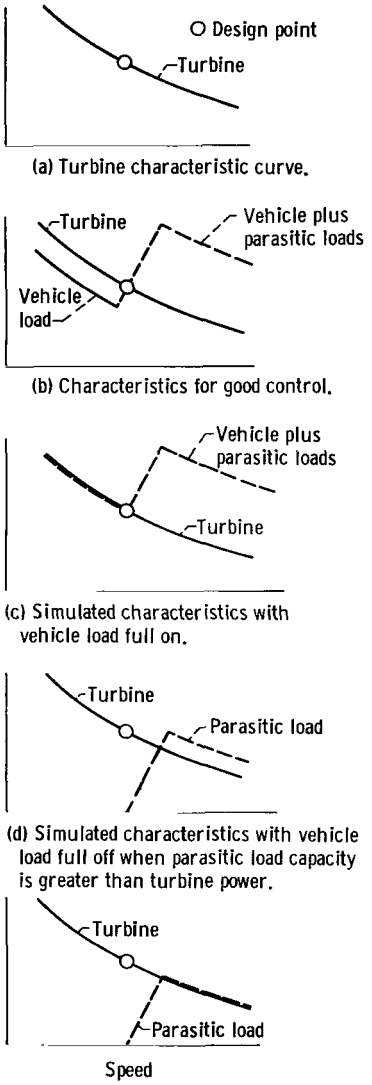

(a) Turbine characteristic curve.

(b) Characteristics for good control.

(c) Simulated characteristics with vehicle load full on.

(d) Simulated characteristics with vehicle load full off when parasitic load capacity is greater than turbine power.

(e) Simulated characteristic with vehicle load full off when parasitic capacity equals turbine power.

Figure 1. - Typical torque-speed curves.

(1) Maximum frequency deviation can be ±2 percent in transient and ±1 percent at steady state from the 400 cps set point.

(2) Recovery time shall be 1 second or less and is defined as the time required for transient speed to return to ±1 percent of the 400 cps set point.

(3) Sustained oscillations in frequency may not occur.

The specifications require that the turboalternator speed be constrained within a narrow range under all operating conditions. Over this range, the estimated power output of the turbine is essentially constant. The turbine torque-speed curve for constant power is shown schematically in figure 1(a). Superimposed on this same curve in figure 1(b) is a load torque-speed curve of the type needed for good speed control; that is, with such a load curve there is a torque difference in either direction from the design point which tends to restore speed to the design value. A load torque-speed curve of the type shown in figure 1(b) can be obtained by use of a controlled parasitic load in conjunction with the vehicle load. Three controller parameters are important in determining the shape of this curve and its position relative to the turbine torque-speed curve. These parameters are (1) the power dissipation capacity of the parasitic load, (2) the total controller gain, and (3) the fraction of the alternator power dissipated by the parasitic load at design operating conditions. The capacity of the parasitic load determines the maximum change in load torque which can be implemented by the speed controller. The total gain, of which the capacity is a factor, determines the slope of the load curve where it crosses the turbine curve, and the fraction of the alternator power dissipated by the parasitic load at design-point conditions determines how far the operative range of the control extends below design speed. These three parameters, plus the controller time constants, are the important factors that determine the performance of the speed control.

Ranges of parasitic-load capacity, total controller

gain, and time constants were considered in the study. For the third parameter, the simulated controller dissipated zero power at design operating conditions. For this parameter to be zero in the real system, of course, would be unsatisfactory, since there would be no control of speed below the design value. However, since only small values of parasitic power at the design point are consistent with desired efficiencies of the Brayton system, it was decided that the study of this control parameter must be accomplished in an experimental investigation of the complete power system.

The load characteristics used in the simulation are shown schematically in figures 1(c), (d), and (e). The general characteristic for applications of vehicle load is given in figure 1(c), while the characteristics for removal of vehicle load are shown in figures 1(d) and (e). Figure 1(e) depicts the special case for which the parasitic capacity was equal to the turbine power (10 kW). The speed is uncontrolled where the load and turbine curves are coincident. Again, this situation would be unsatisfactory in the real system. The study included this special case (fig. 1(e)) for the purpose of providing a broad range of parasitic load capacities in the evaluation of time constant requirements.

Control Description

A simplified flow diagram of the turboalternator, the voltage regulator, the speed control, the parasitic load, and the vehicle load is shown in figure 2. It is assumed that this subsystem can be studied independently of the remainder of the Brayton system, because the power into the turbine remains nearly constant for speed changes near the design point.

A simplified signal-flow diagram of the speed control circuits is shown in figure 3. The turboalternator speed is sensed as alternator line frequency and compared with the

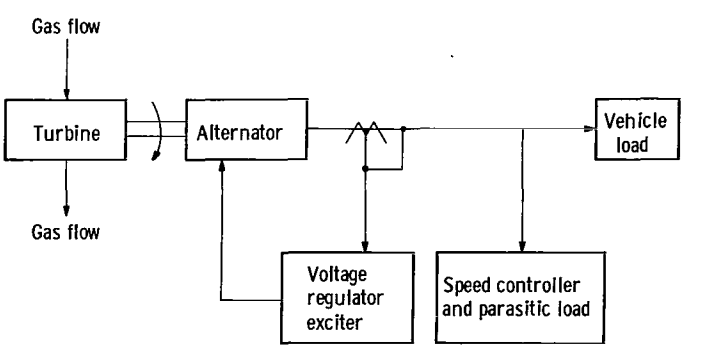

Figure 2. - Turboalternator subsystem.

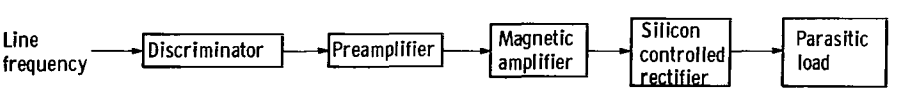

Figure 3. - Simplified speed controller.

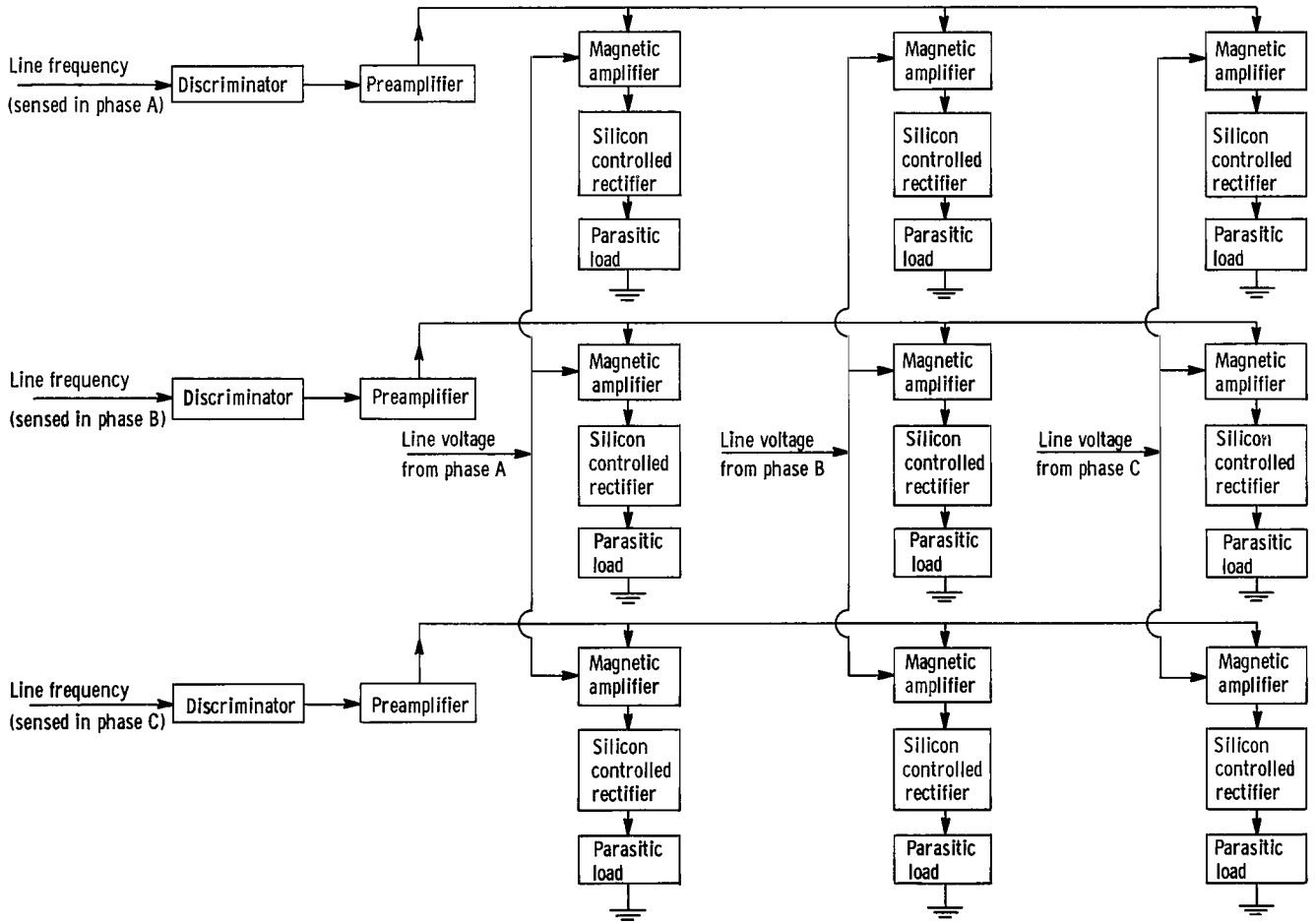

Figure 4. - Speed controller signal flow.

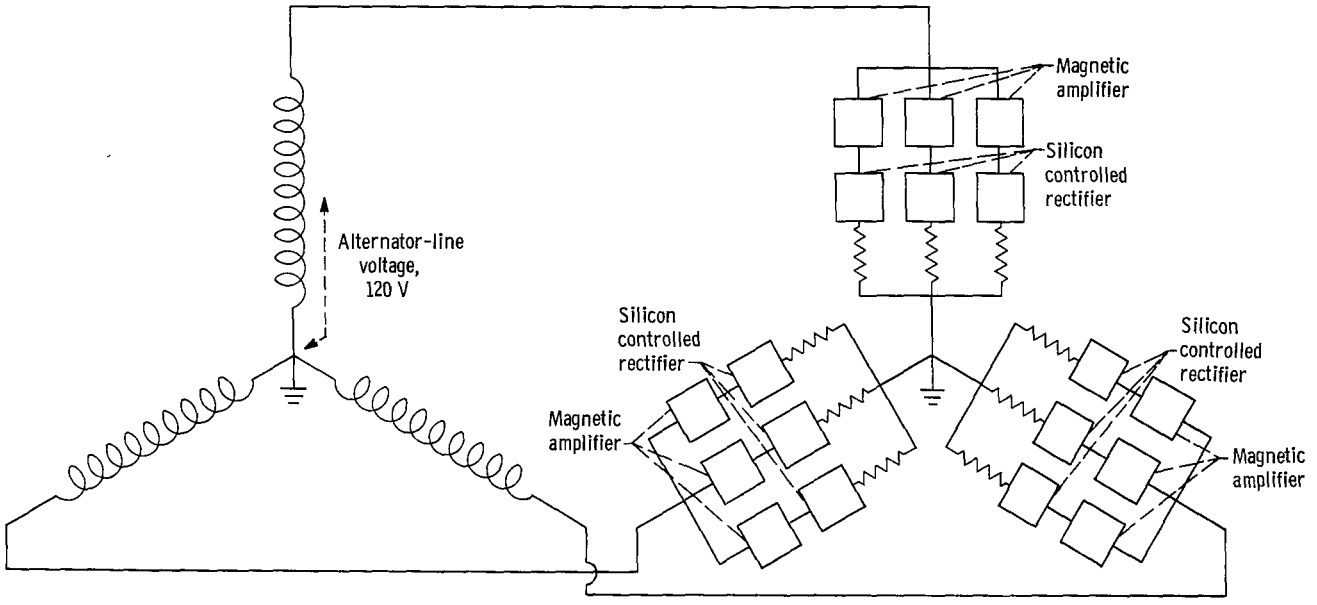

Resistor value	Total parasitic load capacity, kW (line voltage 120 V)
6.18	21
7.20	18
10.80	12
12.96	10

Figure 5. - Parasitic load and alternator circuit.

reference value in the discriminator. For frequencies greater than the reference value, an error signal exists, and the discriminator converts this error into a proportional current, which is then amplified in three stages: the preamplifier, the magnetic amplifier, and the silicon controlled rectifier (SCR) stages. The SCR gate current controls the current flow into the parasitic load, where the power is dissipated through resistive heating.

The speed controller consists of three separate circuits, each of which acts in the manner just described with respect to different reference points. All three circuits are shown in more detail in figure 4. The first circuit has a 400-cps reference and senses frequency in phase A. The second and third circuits have references of 401 and 402 cps and sense frequency in phases B and C, respectively. Each circuit controls three parasitic load resistors and the power to each of the three resistors is supplied by a separate alternator phase (φ_A, φ_B, or φ_C). Therefore, with three control circuits and three parasitic resistors per circuit, there are nine resistors to dissipate power. These resistors are connected as a y-connected load to the y-connected alternator, as shown in figure 5. The resistor value necessary to achieve various total parasitic-load capacities

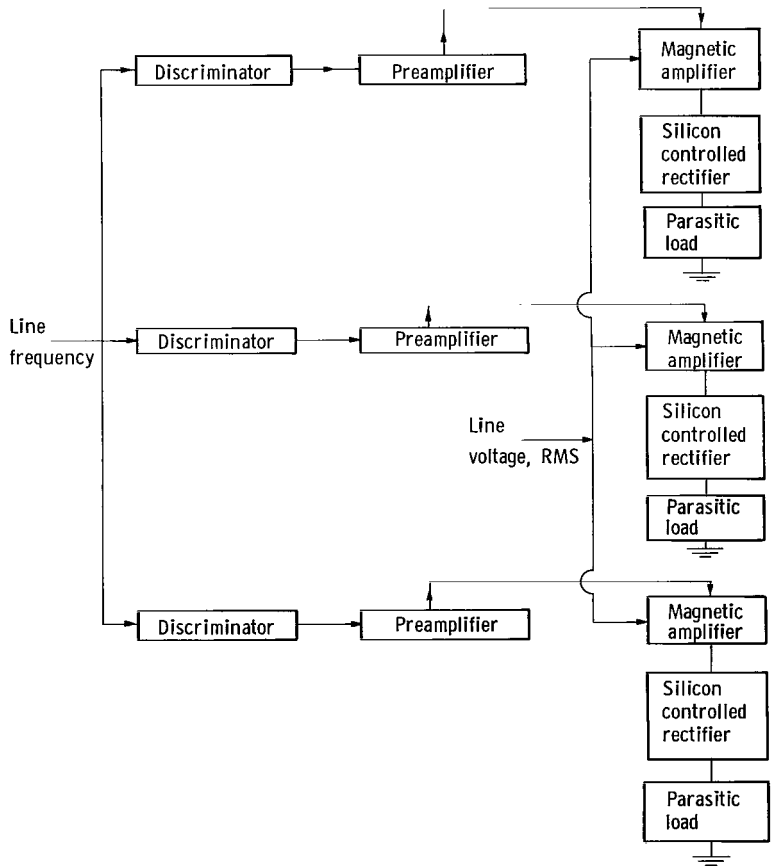

Figure 6. - Signal flow diagram of equivalent speed controller circuits.

is shown in the table in figure 5.

For purposes of simulation, the speed controller circuits of figure 4 can be simplified, since line frequencies and root-mean-square voltages are the same in all phases. In the equivalent circuit in figure 6, the parasitic loads are three times larger than those in figure 4. Other circuit components in figure 6 are the same as the corresponding components in figure 4.

The design range of output variables for the speed controller components is given in table I. As an example, at 400 cps the SCR's of all three control circuits are at a firing angle of 0^{o}. Figure 7 shows that, at a firing angle of 0^{o}, no power is being dissipated in the parasitic loads. For a frequency error of 2 cps (frequency of 402 cps) the SCR's of the 400-cps reference circuit are at a firing angle of 170^{o}, and maximum power dissipation occurs for that particular circuit load. For the same frequency, the 401-cps reference SCR are at a firing angle of 85^{o}, and the power dissipation in the circuit is 45 percent of its maximum value, while the 402-cps control circuit is inactive with 0^{o} SCR firing angle and no power dissipation.

The ranges of variables in table I, figure 7, and the parasitic-load capacity determine the steady-state gains for the speed controller components. These gains, shown on a signal flow diagram of the controller (fig. 8), are defined. Also, several composite gains are defined and are discussed in the following paragraph.

If controller gain is defined as

$$K_c = K_d K_{pa} K_m K_\alpha = \frac{\Delta\alpha}{\Delta e} \qquad \text{(each circuit)}$$

overall controller gain as

TABLE I. - RANGE OF OUTPUT VARIABLES FOR SPEED CONTROLLER COMPONENTS

Frequency of reference circuit, cps	Frequency sensed in alternator phase	Control operative over alternator electrical frequency range, cps	Range of discrimator output current, mA	Range of preamplifier output current, mA	Range of magnetic amplifier output current, mA	Range of silicon controlled rectifier firing angle, deg
400	A	400 to 402	0 to 4	40 to 2	5 to 273	0 to 170
401	B	401 to 403	0 to 4	40 to 2	5 to 273	0 to 170
402	C	402 to 404	0 to 4	40 to 2	5 to 273	0 to 170

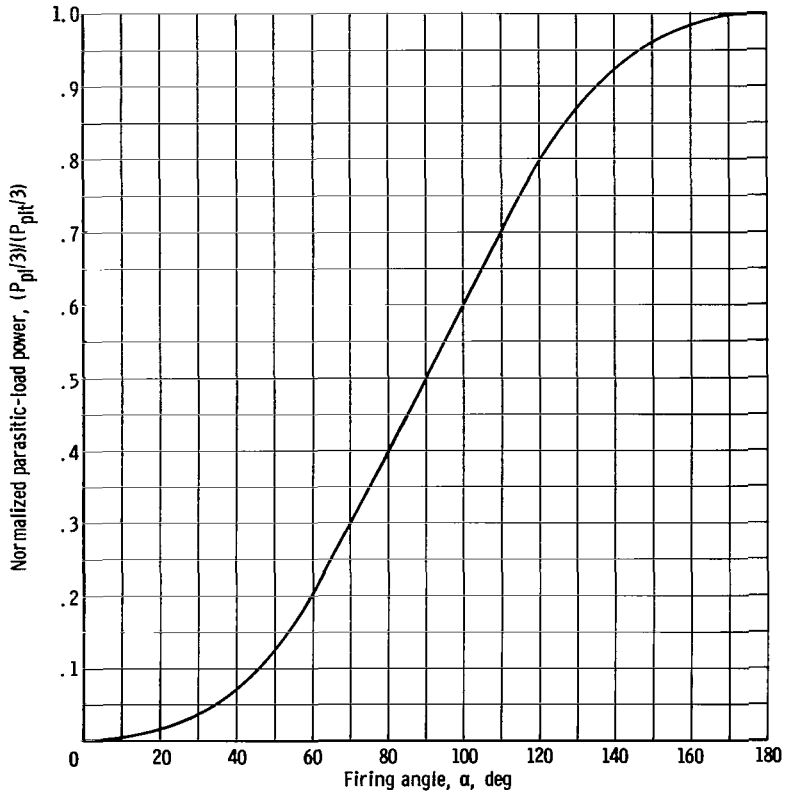

Figure 7. - Normalized parasitic-load power as function of silicon controlled rectifier firing angle.

$$K_0 = K_c K_{pl} = \frac{\Delta(P_{pl}/3)}{\Delta e} \qquad \text{(each circuit)}$$

and total controller gain as

$$K_t = \frac{\Delta P_{pl}}{\Delta f}$$

It can be shown that

$$K_t = 2K_0$$

if $401 \leq f \leq 403$,

$$K_t = K_0$$

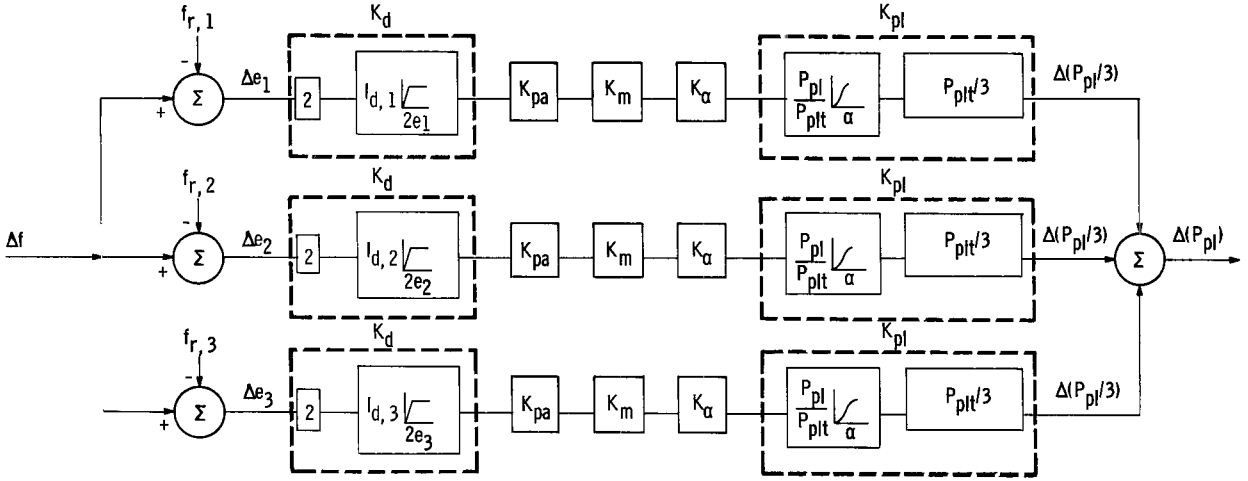

$$K_d = \frac{\Delta(\text{Output discriminator current } I_d)}{\Delta(\text{Frequency error } e)}$$

$$K_{pa} = \frac{\Delta(\text{Output preamplifier current } I_{pa})}{\Delta(\text{Output discriminator current } I_d)}$$

$$K_m = \frac{\Delta(\text{Output magnetic amplifier current } I_m)}{\Delta(\text{Output preamplifier current } I_{pa})}$$

$$K_\alpha = \frac{\Delta(\text{Silicon controlled rectifier firing angle } \alpha)}{\Delta(\text{Output magnetic amplifier current } I_m)}$$

$$K_{pl} = \frac{\Delta(1/3 \text{ of parasitic-load power } P_{pl}/3)}{\Delta(\text{Silicon controlled rectifier firing angle } \alpha)}$$

Figure 8. - Signal flow diagram of steady-state gains in speed controller circuits.

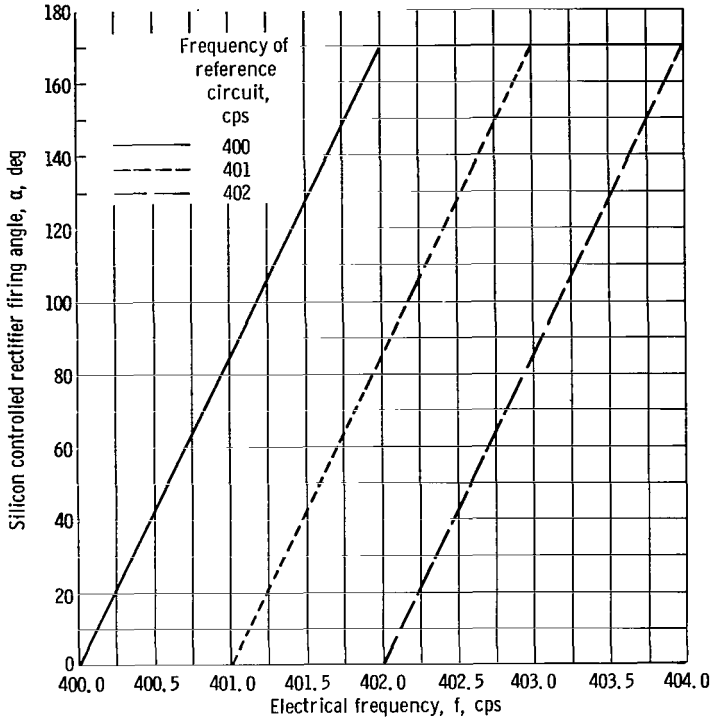

Figure 9. - Silicon controlled rectifier firing angle as function of electrical frequency.

if $400 < f < 401$ or $403 < f < 404$, and

$$K_t = 0$$

for all other frequencies. The SCR firing angle as a function of alternator frequency is shown in figure 9 for each individual speed controller circuit. The end points of the curves are the values given in table I. The slope of each curve (85 deg/cps) is the gain of SCR firing angle to frequency error. This gain K_c is designated controller gain. There is one other stage of gain K_{pl} in each control circuit. This gain is determined by the relation between parasitic-load power consumption and SCR firing angle and is, therefore, dependent on the resistor value used. The overall gain $K_0(K_0 = K_c K_{pl})$ for each control circuit is given by the slopes of the three similar curves in figure 10(a) for an 18-kilowatt-capacity parasitic load. Adding the ordinates of the three curves together, frequency by frequency, yields the total parasitic-load power as a function of frequency (also shown in fig. 10(a)); the slope of this curve (6000 W/cps in the linear range) is the total controller gain K_t for an 18-kilowatt-capacity parasitic load. This 18-kilowatt-capacity curve is also shown in figure 10(b) along with similar curves for 12- and 10-kilowatt parasitic loads. Figure 10(b) shows that the 12- and the 10-kilowatt parasitic

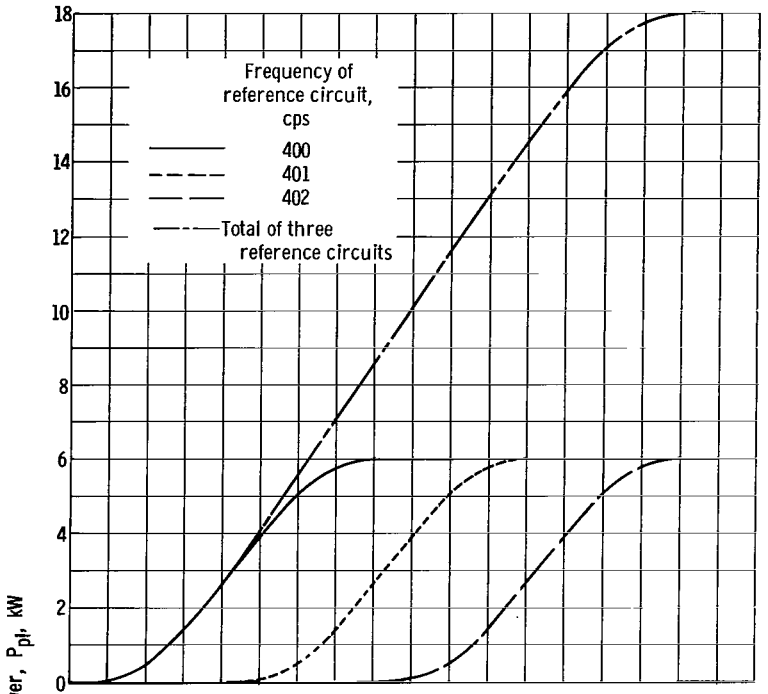

(a) Parasitic-load capacity, 18 kilowatts.

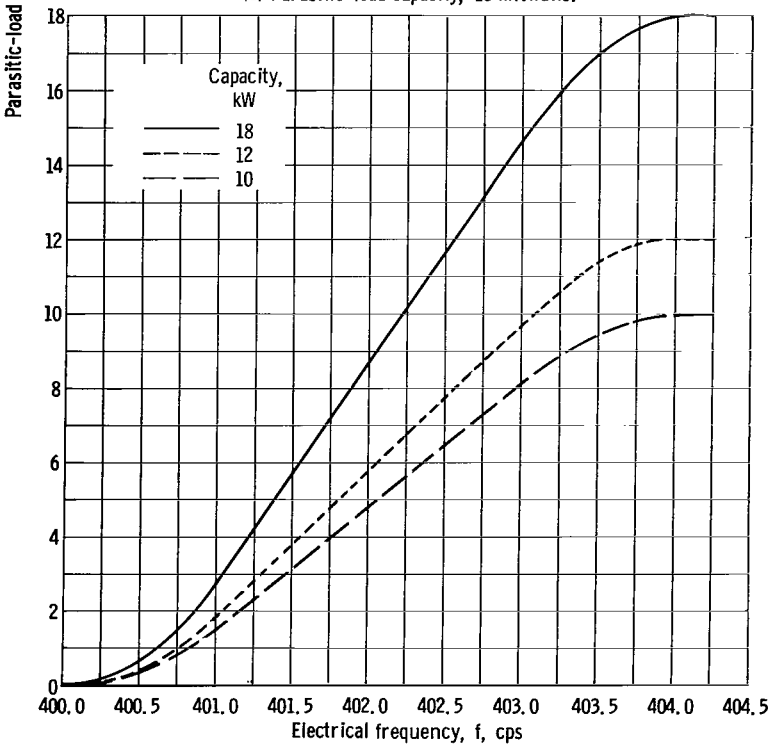

(b) Various parasitic-load capacities.

Figure 10. - Parasitic-load power as function of electrical frequency.

loads have total gains of 4000 and 3400 watts per cps, respectively, in their linear ranges.

Simulation

The dynamics of the turboalternator and the speed control were represented by equations (1) to (13). In this group of equations, equations (1) to (4) represent the turboalternator, and equations (5) to (13) represent the components of the speed-control circuits. With the exception of equation (12), all the speed-control equations are the same for each of the three circuits. In equation (12), the reference values are different for the three control circuits. The values of the constants in the equations are given in the list of constants following the equations. (All symbols are defined in the appendix.)

$$T_T - T_l = 2\pi \mathscr{I} \frac{dN}{dt} \tag{1}$$

$$T_T = \frac{P_t}{2\pi \frac{746}{550} N} \tag{2}$$

where P_t is in watts.

$$T_l = \frac{P_{vl} + P_{pl,1} + P_{pl,2} + P_{pl,3}}{2\pi \frac{746}{550} N} \tag{3}$$

$$P_{vl} = K_1 V_{ln}^2 \tag{4}$$

where

$$K_1 = \frac{P_{vl,\,design}}{V_{ln,\,design}^2}$$

$$P_{pl,i} = \frac{P_{plt}}{3}\left(\frac{P_{pl}}{P_{plt}}\right)_i \qquad i = 1, 2, 3 \tag{5}$$

$$\frac{P_{plt}}{3} = K_2 V_{ln}^3 \tag{6}$$

where

$$K_2 = \frac{P_{plt,\,design}/3}{V_{ln,\,design}^2}$$

$$\frac{P_{pl}}{P_{plt}} = f(\alpha) \qquad \text{(fig. 7)} \tag{7}$$

$$\alpha = K_\alpha (I_m - I_{m,0}) \tag{8}$$

$$I_m - I_{m,0} = \frac{K_m}{1 + \tau_m S}(I_{pa} - I_{pa,0}) \tag{9}$$

$$I_{pa} - I_{pa,0} = \frac{K_{pa}}{1 + \tau_{pa} S} I_d \tag{10}$$

$$I_d = K_d e \tag{11}$$

$$e_i = f - f_{r,i}, \quad i = 1, 2, 3 \tag{12}$$

where $f_{r,1}$ is 400 cps, $f_{r,2}$ is 401 cps, and $f_{r,3}$ is 402 cps.

$$f = \frac{p}{2} N \tag{13}$$

The values of the constants in the preceding equations, listed in order of their occurrence, are as follows:

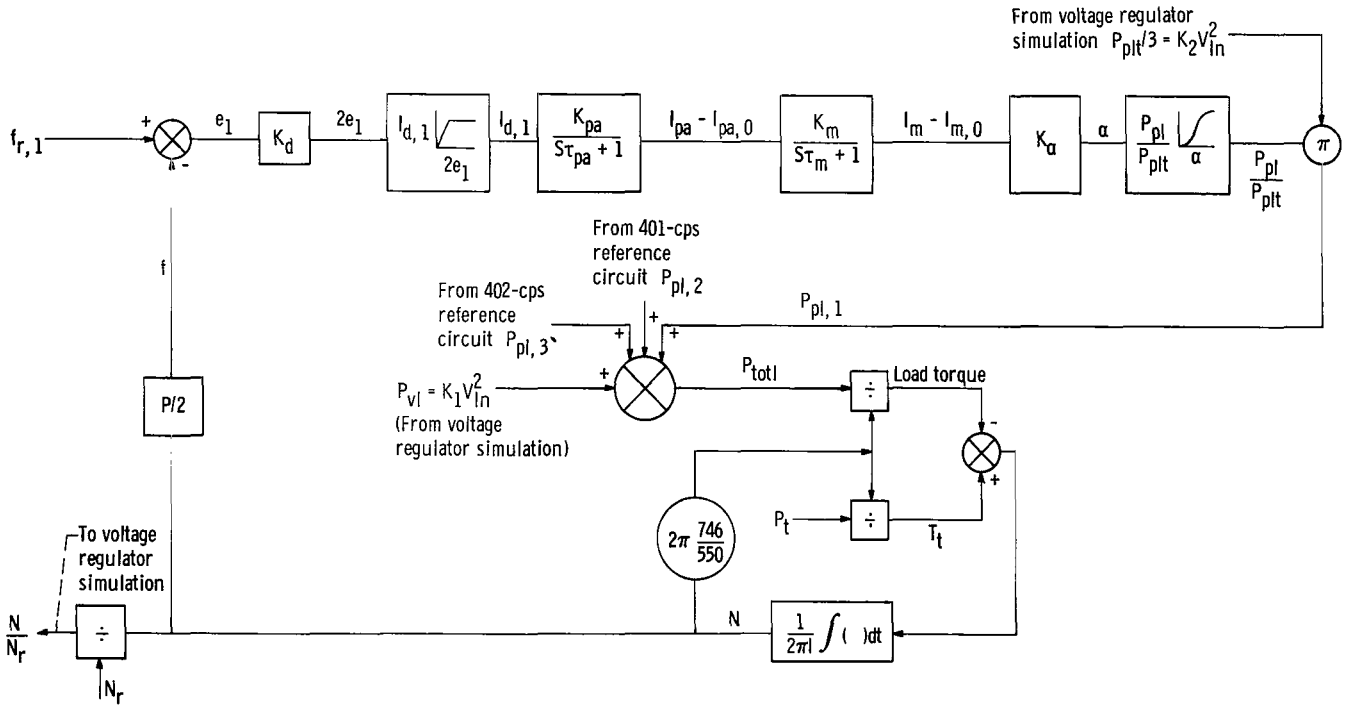

Figure 11. - Simulated turboalternator subsystem. (Two speed control circuits are not shown.)

Inertia of turboalternator, $\mathcal{I}$, (ft-lb)(sec^2)	0.051
Turbine power, P_t, W	10 000
Constant, C_1, W/V^2	0.694
Constant, C_2, W/V^2, for maximum power that can be dissipated by parasitic load, P_{plt}, of	
10 kW	0.232
12 kW	0.278
18 kW	0.417
Gain of silicon controlled rectifier, K_α, deg/mA	0.635
Magnetic amplifier output current for e = 0, $I_{m,0}$, mA	5
Gain of magnetic amplifier, K_m	-7.05
Preamplifier output current for e = 0, $I_{pa,0}$, mA	40
Gain of preamplifier, K_{pa}	-9.5
Discriminator gain, K_d, mA/cps	2
Number of poles, p	4

As mentioned previously, the turbine-output power is essentially constant over the range of speed under consideration. In the simulated relation between turbine torque and speed represented by equation (2), the power P_t is thus a constant 10 kilowatts. The alternator electrical efficiency was assumed to be 100 percent. Thus the sum of the vehicle and parasitic-load powers in equation (3) at steady state is 10 kilowatts.

A block diagram of the speed control and turboalternator (excluding the voltage regulator) is shown in figure 11, as simulated on the analog computer. A 10-kilowatt-capacity vehicle load (for a line voltage of 120 V) was used. The preamplifier and the magnetic amplifier time constants were assumed to have the same values for load-off as for load-applied transients. Saturation of controller components was simulated by use of a diode circuit. The parasitic-load power as a function of SCR firing angle (fig. 7, p. 9) was simulated by means of a diode function generator.

The effect of the voltage-regulator dynamics on the speed control performance is also included in the simulation. A block diagram of the voltage regulator simulation is shown in figure 12. The closed-loop transfer function (eq. (14)) can be obtained directly from this figure. The values of the gains in equation (14) are given in figure 12.

$$\frac{V_{ln}}{V_r} = \frac{\frac{N}{N_r} K_1 G_1 G_2}{1 + K_2 K_1 G_1 G_2 \frac{N}{N_r}} \tag{14}$$

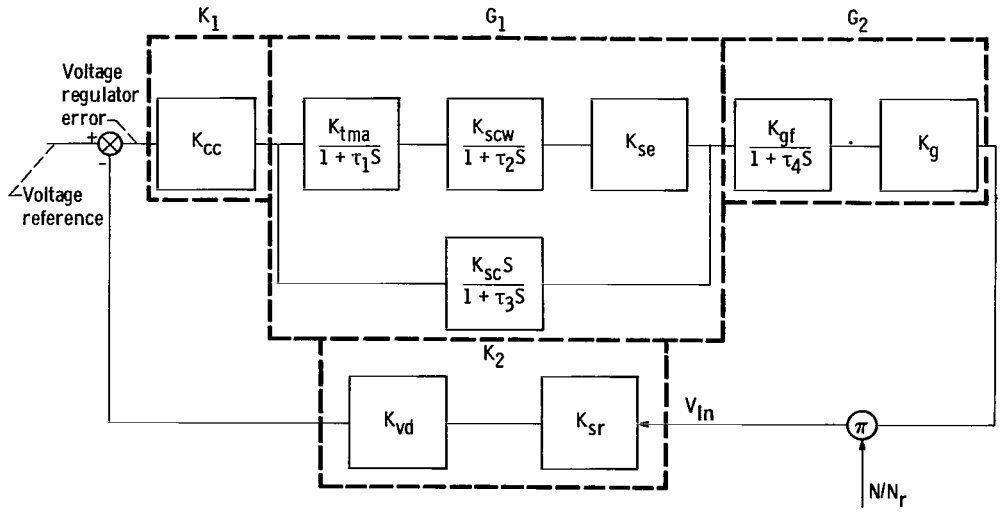

Comparison circuit gain, K_{cc}	1/6000
Transistor magnetic amplifier, K_{tma}	1.26×10^{4}
Gain of saturable current potential transformer control winding, K_{scw}	1
Static exciter gain, K_{se}	25
Generator field gain, K_{gf}	0.2
Generator gain, K_g	36.3
Stabilizing circuit gain, K_{sc}	3×10^{-7}
Gain of voltage divider, K_{vd}	11.7/135
Gain of sensitizing rectifier, K_{sr}	135/120
Time constants, sec,	
τ_1	0.07
τ_2	0.01
τ_3	0.18
τ_4	0.17

Figure 12. - Voltage regulator and alternator simulation.

where

$$K_1 = \frac{1}{6000}$$

$$G_1 = \frac{\dfrac{K_{tma}K_{scw}K_{se}}{(1+\tau_1 S)(1+\tau_2 S)}}{1 + \dfrac{K_{tma}K_{scw}K_{se}K_{sc}S}{(1+\tau_1 S)(1+\tau_2 S)(1+\tau_3 S)}}$$

$$G_2 = \frac{K_{gf}K_g}{1+\tau_4 S}$$

$$K_2 = K_{vd}K_{sr}$$

The voltage regulator functions by manipulation of the alternator field current and includes a stabilizing circuit. As shown in the figure, the following values were used for the time constants of equation (14): $\tau_1 = 0.07$, $\tau_2 = 0.01$, $\tau_3 = 0.18$, and $\tau_4 = 0.17$ seconds. These time constants, as well as the gains used, are the values at the no-load condition.

Line voltage is a function of normalized speed (eq. (14) and fig. 12). This function represents the direct interaction of shaft speed with alternator-output voltage.

Simulated Tests

The investigation was conducted for design and off-design control parameters by stepping a 10-kilowatt vehicle load off, allowing the system to reach steady state, and then stepping the vehicle load back on. Appropriate runs were made to determine the following effects:

(1) The effect of parasitic-load capacity on steady-state and maximum transient speed error with controller gain and time constants at design value

(2) The effect of various preamplifier and magnetic amplifier time constants on speed recovery time, maximum transient error, overshoot, and damped frequency

(3) The effect of controller gain and time constants on the range of stable operation

(4) Interaction of the speed control with an unstable voltage regulator

RESULTS AND DISCUSSION

Performance as Function of Parasitic-Load Capacity

The transient speed responses for the stepwise removal and application of the 10-kilowatt vehicle load for 10-, 12-, and 18-kilowatt parasitic-load capacities are shown in figure 13 for design values of controller gains and time constants. This figure shows that the speed overshoot (of the final steady-state value) is zero for the 10-kilowatt parasitic-load capacity and small for the 12- and 18-kilowatt capacities following removal of a 10-kilowatt vehicle load. Upon reapplication of the vehicle load, speed does not overshoot its final value, and its final value is the control set point. This statement is true for all three parasitic loads. Because the control set point was made equal to the turboalternator design speed, both steady-state and transient speed errors are zero for the stepwise application of full (10 kW) vehicle load.

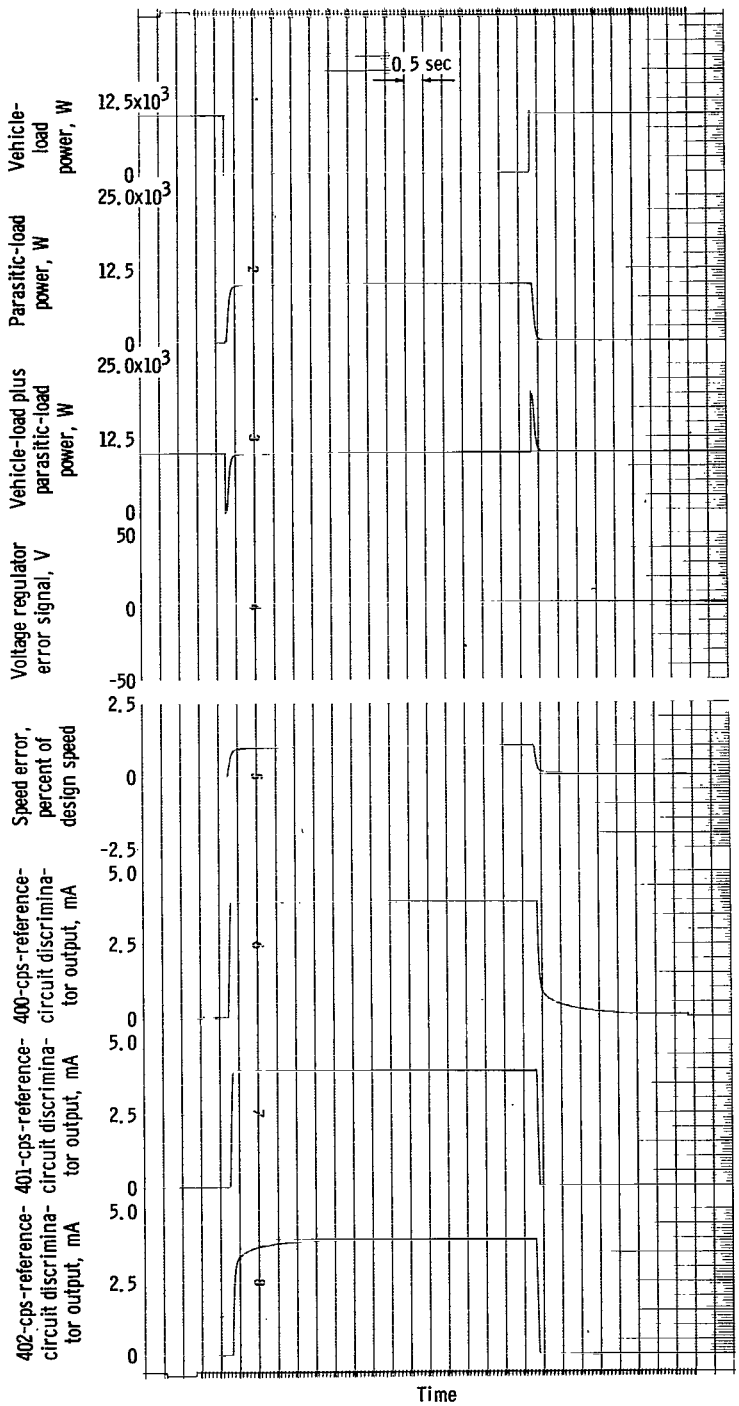

(a) Parasitic load capacity, 10 kilowatts.

Figure 13. - Response of system variables to stepwise removal and application of 10-kilowatt vehicle load for design time constants.

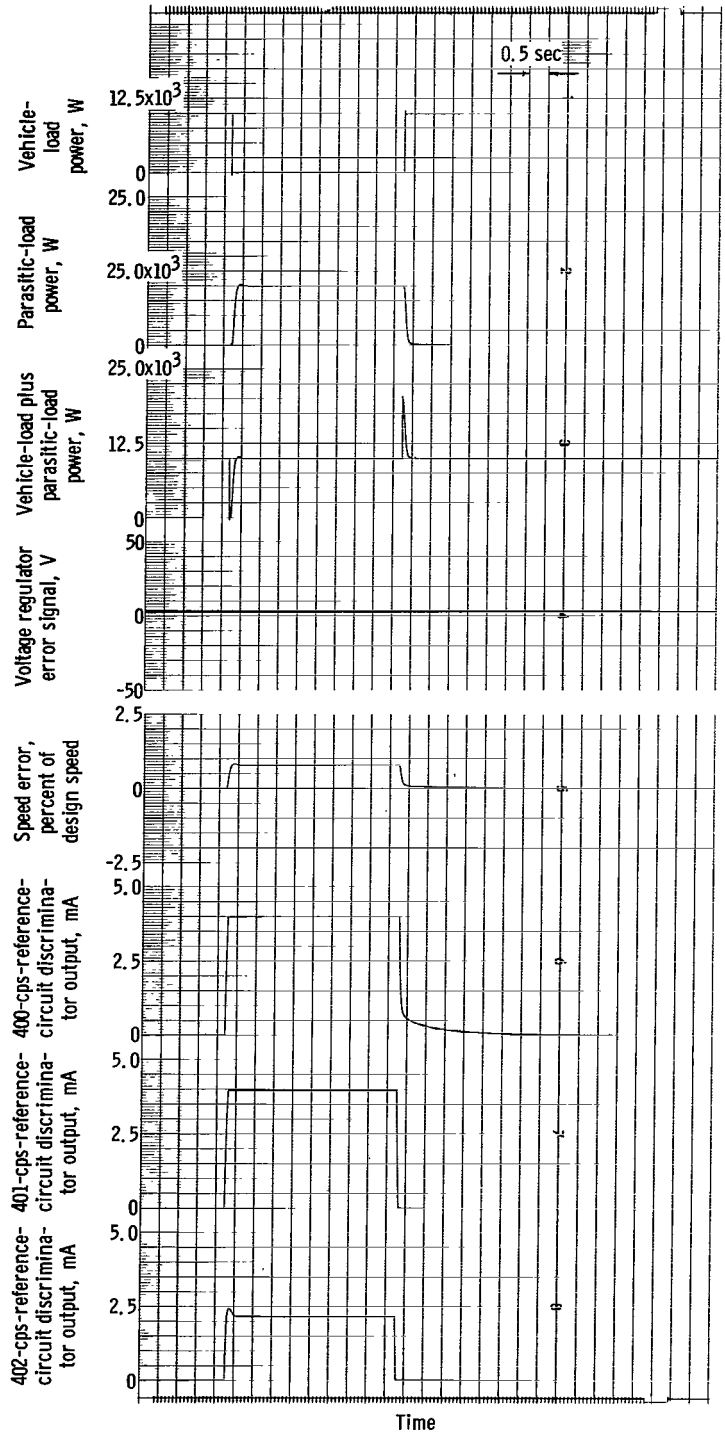

(b) Parasitic load capacity, 12 kilowatts.

Figure 13. - Continued.

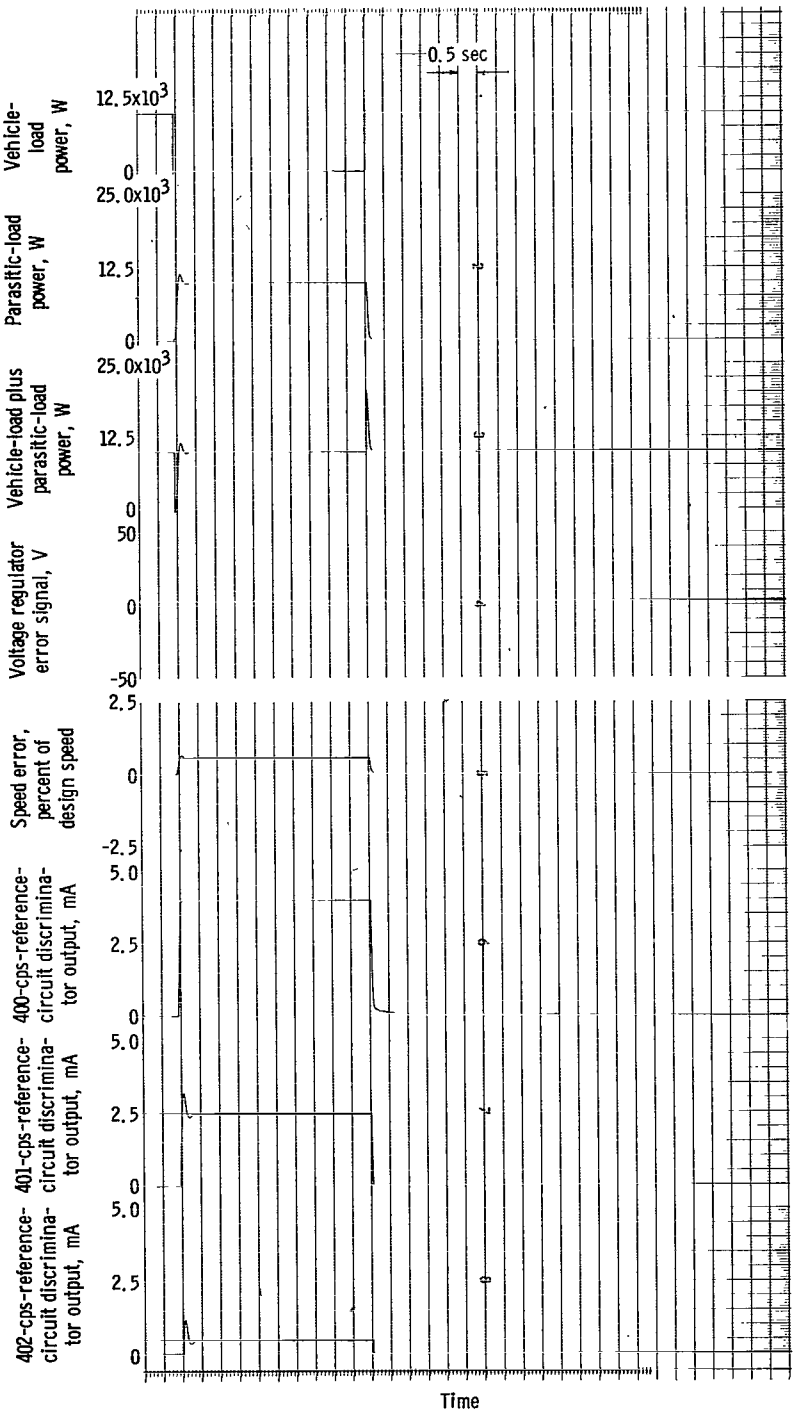

(c) Parasitic load capacity, 18 kilowatts.

Figure 13. - Concluded.

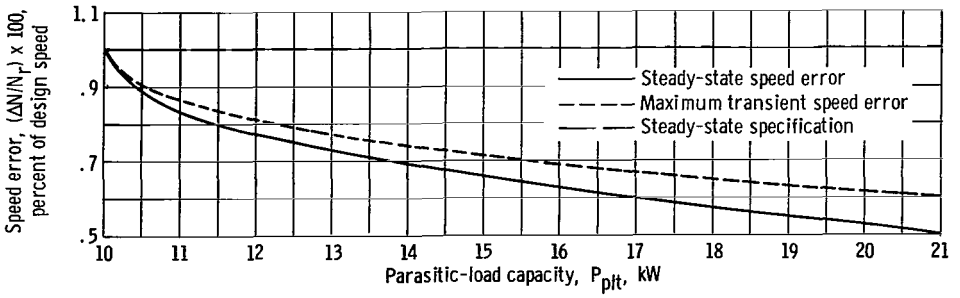

Figure 14. - Steady-state and maximum transient speed error as functions of parasitic-load capacity for stepwise removal of vehicle-load with design values of controller gains and time constants.

The speed errors for the load-removal transient are shown in figure 14 as a function of parasitic load. The inverse variation of speed error with parasitic-load capacity shown in this figure is explained, of course, by the fact that overall control gain increases with increasing capacity (fig. 10(b)). Steady-state speed error is smaller than the allowed variation of 1 percent from the 400-cps condition for parasitic-load capacities greater than 10 kilowatts, and it is equal to the 1 percent allowance for the 10-kilowatt value of parasitic capacity. Also, maximum transient speed error is less than 1 percent for capacities greater than 10 kilowatts and is equal to 1 percent for a 10-kilowatt capacity; therefore, recovery time, by definition, is zero for all capacities studied at design controller gains and time constants.

For the transients studied (figs. 13 and 14), it can be concluded that, with design values of controller gains and time constants, the simulated speed control satisfies the specifications with parasitic-load capacities equal to or greater than the design turboalternator output of 10 kilowatts. In a real system, however, the parasitic-load capacity should be larger than the power output of the turboalternator in order to ensure positive control when the vehicle load is off.

One important factor to be gained with larger capacity is reduction of Joule heating. The discriminator in the 400-cps reference circuit (fig. 15) yields maximum output current (4 mA) for all parasitic capacities less than 20 kilowatts during steady-state operation with no vehicle load, but the 401-cps reference discriminator operates in a saturated state only for capacities less than about 12 kilowatts. The discriminator in the 402-cps circuit does not saturate for capacities greater than 10 kilowatts. For parasitic-load capacities above about 12 kilowatts, therefore, the 401- and the 402-cps circuits are not turned on fully for the no-vehicle-load condition. Joule heating is thus reduced in the 401- and the 402-cps circuits.

Larger capacities also provide sufficient redundancy such that malfunction of one control circuit leaves the parasitic load with sufficient capacity to control the speed within the steady-state specification. With a total parasitic capacity of 18 kilowatts, for example, loss of the resistors in one circuit would leave a dissipative capacity of 12 kilowatts.

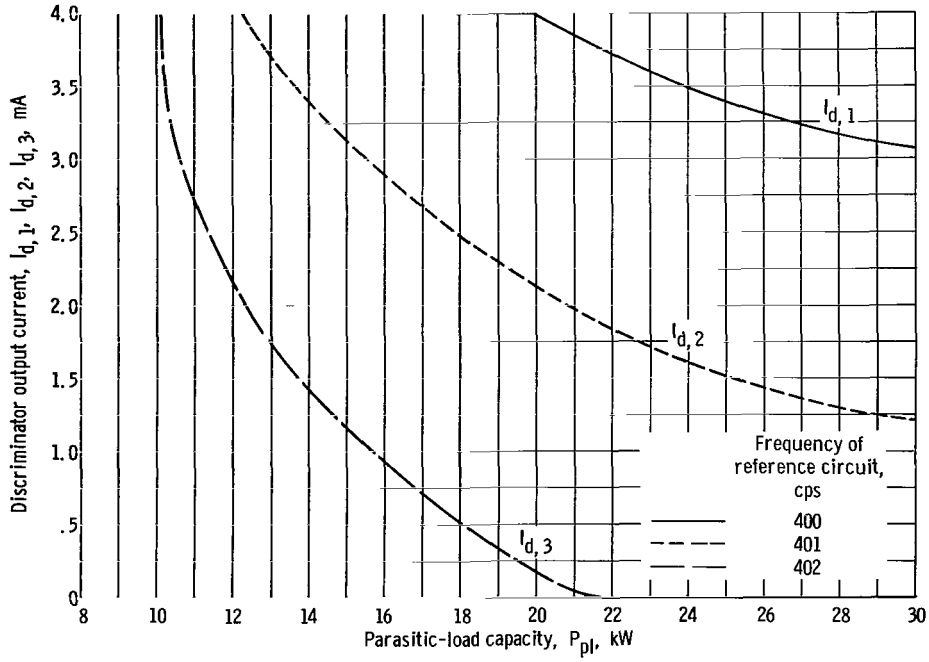

Figure 15. - Discriminator-output current as function of parasitic-load capacity for no vehicle load.

Further study, however, would be required to determine whether or not the transient and stability specifications could be satisfied by such a circuit.

Still another factor suggests the use of the larger capacities. Reference 2 indicates that turboalternator power may reach 18 kilowatts during the startup of the Brayton system unless a special control is provided. (This high power results from low compressor-inlet temperatures due to an initially cold radiator.) Parasitic capacities capable of handling this overpower condition would thus eliminate the added complexity of an additional system control.

Performance as Function of Controller Time Constants

The effect of off-design values of control time constants on the speed response to stepwise removal and application of vehicle load is discussed in this section. Parasitic-load capacities of 10, 12, and 18 kilowatts were studied. The objective was to determine the range of time constants over which speed response remains within specifications.

The results of the study is first presented in the form of correlations between speed response variables (maximum transient error, recovery time, and steady-state error) and magnetic amplifier and preamplifier time constants. The correlations for the load-

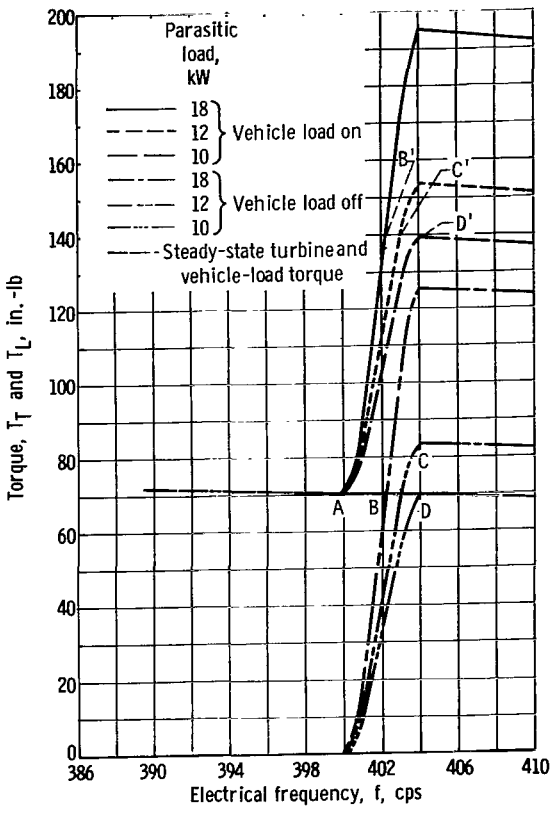

Figure 16. - Steady-state torque as function of electrical frequency.

off transients are considered for each of the parasitic loads, and then those for the load-on transients are discussed. Finally, these correlations are used to determine the ranges of time constants over which the specifications on maximum transient speed, steady-state speed, and recovery time are simultaneously satisfied.

The following facts concerning the load-off transients should be mentioned. If the turboalternator system is operating at its design point (point A in fig. 16), stepwise removal of the vehicle load results in a speed transient until another steady-state point is reached, at which load torque equals applied torque. For parasitic loads greater than 10 kilowatts, the speed will, in general, oscillate about the new steady-state operating point before it settles out with a magnitude and time of oscillation dependent upon the control gain and time constants. These steady-state operating points are dependent upon total controller gain and will always be at the stable intersections of the load curves with the driving-torque curves. These intersections are marked in figure 16 as points B and C for the 18- and the 12-kilowatt parasitic loads, respectively. The 10-kilowatt parasitic load is a special case for which the simulation, with vehicle load off, can operate in steady state at point D or at any point on the curve to the right of D, since there is no net torque in this region. For this case, when the vehicle load is removed, the speed will increase until the parasitic load is fully on, and there will be no restoring action if the steady-state speed tolerance is exceeded. The final speed is thus dependent upon control time constants for a parasitic capacity of 10 kilowatts. Evaluation of the 10-kilowatt parasitic capacity was based solely on whether or not this final speed was within the 1-percent specification. As mentioned previously, a parasitic capacity as small as 10 kilowatts is not recommended for a 10-kilowatt turboalternator. This capacity was used in the simulation as a limiting case in the time-constant study; that is, controls with parasitic capacities that approach this value will have similar time-constant requirements. Otherwise, the specified steady-state speed will not be obtained within the allowable recovery time.

The correlations obtained between maximum transient speed error and magnetic amplifier time constant for several preamplifier time constants is shown in figure 17(a)

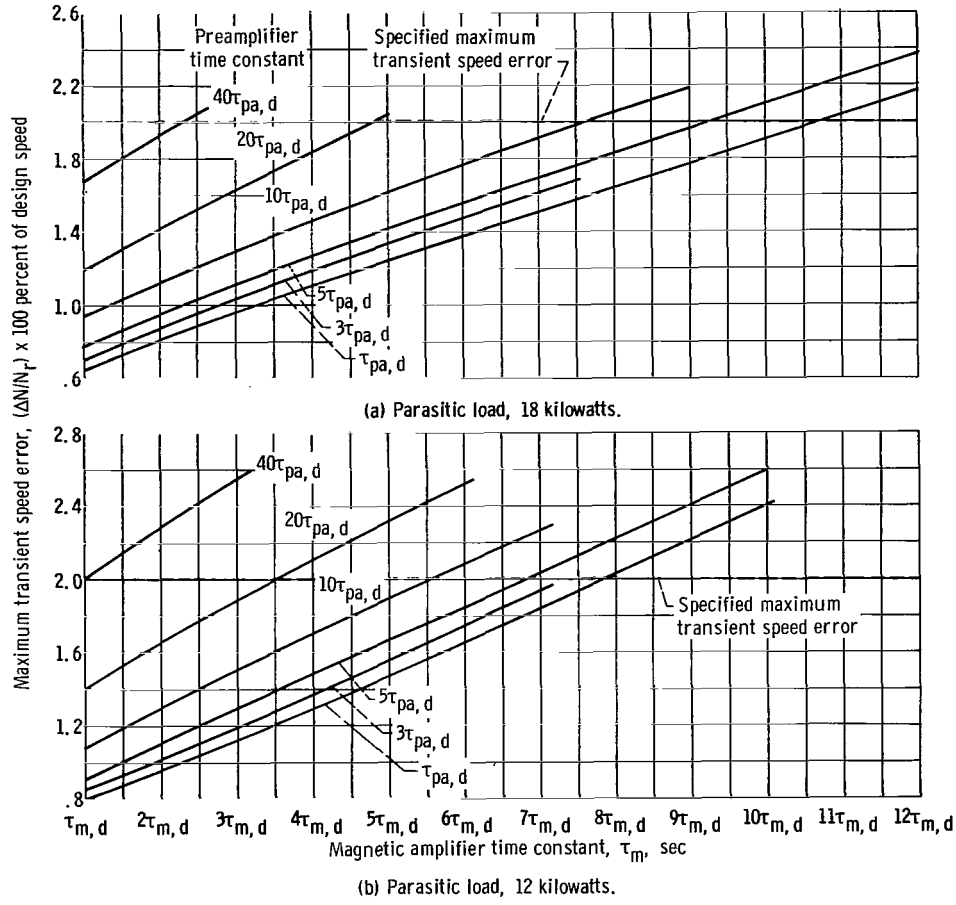

Figure 17. - Maximum transient speed error as function of magnetic amplifier time constant for several preamplifier time constants. Magnetic amplifier design time constant $\tau_{m,d}$, 0.031 second; preamplifier design time constant $\tau_{pa,d}$, 0.005 second; vehicle-load-off transient, 10 kilowatts.

for an 18-kilowatt-capacity parasitic load. The horizontal dashed line represents the 2-percent maximum specified for transient speed. When the preamplifier time constant is equal to its design value (fig. 17(a)), the magnetic amplifier time constant can be almost 11 times its design value (0. 341 sec) before the 2-percent maximum is exceeded. If the parasitic-load capacity is reduced to 12 kilowatts (fig. 17(b)) and the preamplifier time constant is kept at the design value, the 2-percent specification restricts the magnetic amplifier constant to less than eight times its design value (0. 248 sec). With a design magnetic amplifier time constant and a 12-kilowatt-capacity parasitic load, the preamplifier constant can range to 40 times its design value (0. 2 sec); increasing the parasitic capacity to 18 kilowatts increases the allowable preamplifier time constant range above 40 times design.

For the same two parasitic loads (18 and 12 kW), the correlations of recovery time with time constants for the load-off transients are shown in figures 18(a) and (b), respec-

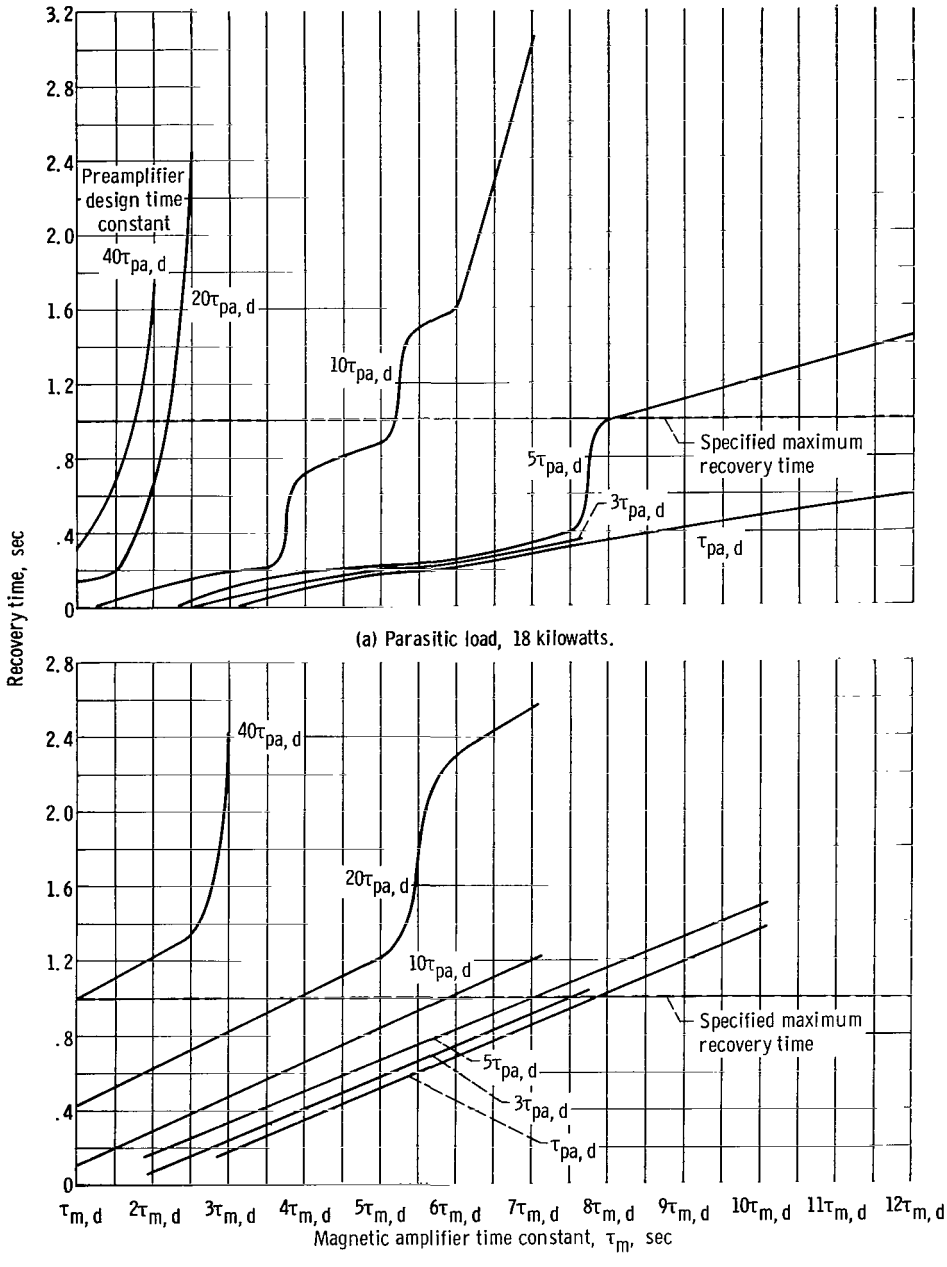

Figure 18. - Recovery time as function of magnetic amplifier time constant for several preamplifier time constants. Magnetic amplifier design time constant $\tau_{m,d}$, 0.031 second; preamplifier design time constant $\tau_{pa,d}$, 0.005 second; vehicle-load-off transient, 10 kilowatts.

tively. The irregularity of some of these curves is due to changes in the number of oscillations that take the speed above the 1-percent criterion upon which recovery time is based. The limits on time-constant variation for the 12-kilowatt parasitic load are nearly the same for both the maximum transient error and the recovery time. This statement does not hold for the 18-kilowatt parasitic load.

The correlations between final speed and control time constants with the vehicle load off for a 10-kilowatt-capacity parasitic load are shown as solid lines in figure 19(a). For design controller time constants, figure 14 shows that the final speed after vehicle-load removal is 1 percent greater than the design value (corresponding to point D in fig. 16). Increasing the magnetic amplifier time constant while keeping the preamplifier time constant at the design value results in a speed error greater than 1 percent (corresponding to points on the curve to the right of D in fig. 16). With the design magnetic-amplifier time constant, the preamplifier constant cannot be increased by more than a factor of three without increasing the speed error above 1 percent (fig. 19(a)).

For stepwise application of the 10-kilowatt real load, each of the parasitic-load controls reacts in a similar manner. For the 18-, 12-, and 10-kilowatt parasitic-load controls with systems operating at points B, C, and D in figure 16, respectively, stepwise application of the vehicle load results in instantaneous changes in the respective load torques to points B', C', and D' on the curves for the combined load torques. For each of these curves, a net speed-decreasing torque exists for frequencies above 400 cps; therefore, in each case, the steady-state condition will be the design point A, or, in the simultation, some point on the curve to the left of A dependent on the control time constants. Again, the assumption is made that simulated errors greater than 1 percent in final speed are unsatisfactory. If a 1-percent error is exceeded, the recovery time would be excessive for a control with small parasitic power dissipation at design condition. The correlations for the load-on transient between final operating speeds and time constants for 10-, 12-, and 18-kilowatt parasitic capacities are shown in figure 19(a), (b), (c). Over the range of time constants common to all three plots, the speed errors for all three parasitic loads are within about 0. 1 percent of each other for a given set of time constants. For both 12- and 18-kilowatt parasitic loads (figs. 19(b) and (c)), the magnetic amplifier time constant can range up to $7\tau_{m,d}$ (0. 217 sec) with design preamplifier time constant, and the preamplifier time constant can exceed $20\tau_{pa,d}$ (0. 01 sec) with design magnetic amplifer time constant before the 1-percent specification is exceeded.

With the correlations presented, it is possible to determine the range of time constants for the 12- and 18-kilowatt parasitic loads over which the three specifications on maximum transient speed, steady-state speed, and recovery time are simultaneously satisfied. For capacities approaching 10 kilowatts, it has already been shown that the allowable time-constant range is small.

For an 18-kilowatt capacity parasitic-load speed control, the percentage maximum-

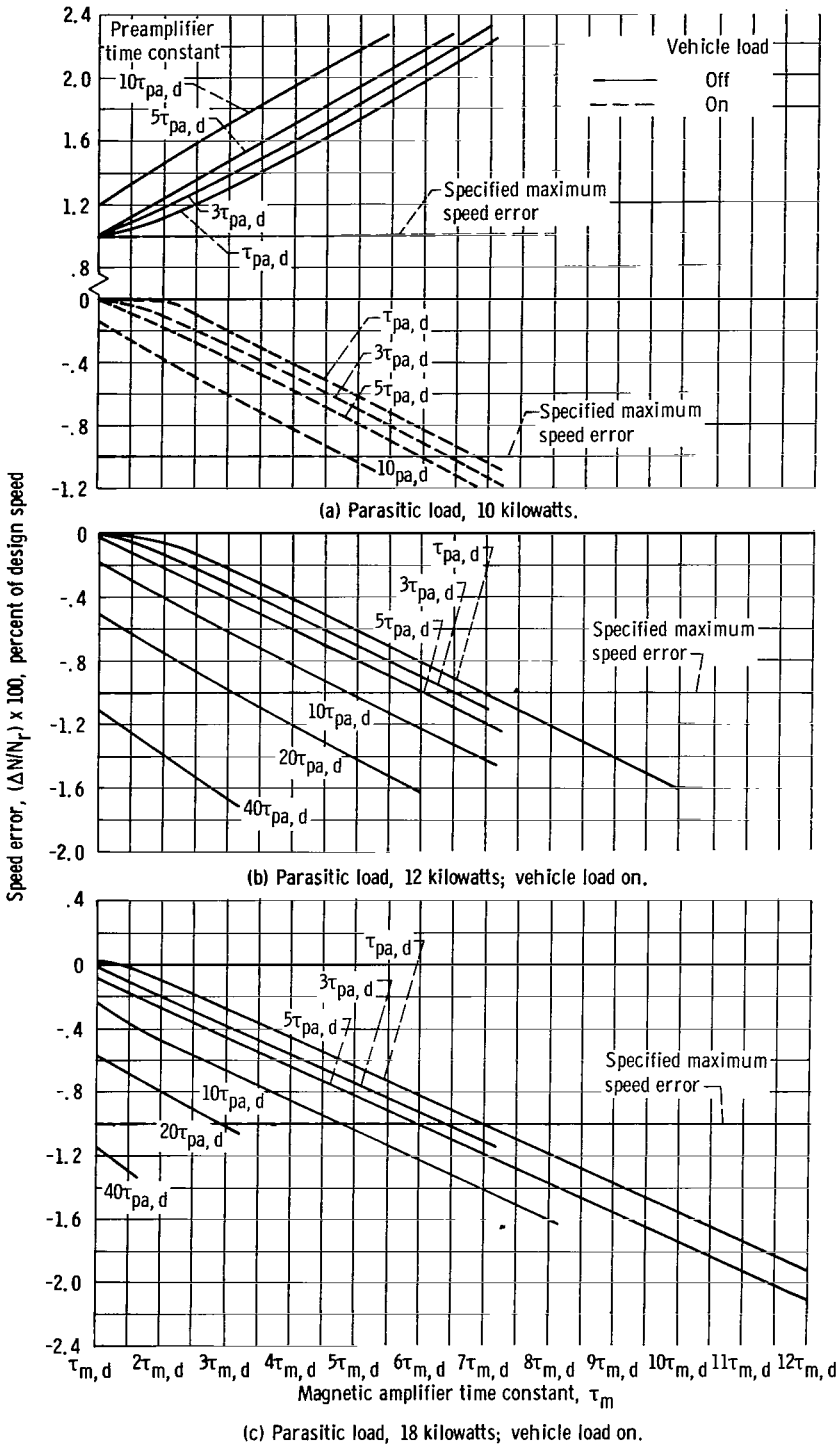

(a) Parasitic load, 10 kilowatts.

(b) Parasitic load, 12 kilowatts; vehicle load on.

(c) Parasitic load, 18 kilowatts; vehicle load on.

Figure 19. - Speed error as function of magnetic amplifier time constant for several preamplifier time constants. Magnetic amplifier design time constant $\tau_{m,d}$, 0.031 second; preamplifier design time constant $\tau_{pa,d}$, 0.005 second.

transient-speed-error and recovery-time correlations with time constants for the vehicle-load-off transient (figs. 17(a) and 18(a), respectively) and the percentage speed-error correlation for vehicle-load on (fig. 19(c)) yield the information required to determine the allowable range of time constants. Comparison of the time-constant ranges which satisfy each of the three specifications is facilitated by plotting a time-constant boundary for each specification on a graph of magnetic amplifier time constant as a function of preamplifier time constant. Such a comparison has been made in figure 20(a) for an 18-kilowatt capacity parasitic load. The information required to draw the recovery-time specification boundary for vehicle load on, for example, was obtained from the correlations of figure 19(c). This information is in accordance with the assumption that speed errors above 1 percent in the simulation imply excessive recovery time in the real situation. The curves of figure 19(c) intersect the 1-percent maximum error line at five points. These five points were replotted in figure 20(a) and connected by a smooth curve to yield the aforementioned boundary. The other two boundaries were obtained in a similar manner from the maximum-transient-speed-error and recovery-time correlations of figures 17(a) and 18(a), respectively. The allowable time-constant range is then indicated by the area lying under all three boundaries.

Similarly, the acceptable range of time constants for a 12-kilowatt parasitic-load control is determined in figure 20(b). The information required to draw the figure was obtained from the correlations of figures 17(b), 18(b), and 19(b).

A comparison of the allowable ranges of time constants at values less than $20\tau_{pa,\,d}$ (which is as far as the recovery-time specification boundary for vehicle-load on was determined) shows that the recovery-time specifications for the vehicle-load-on transient

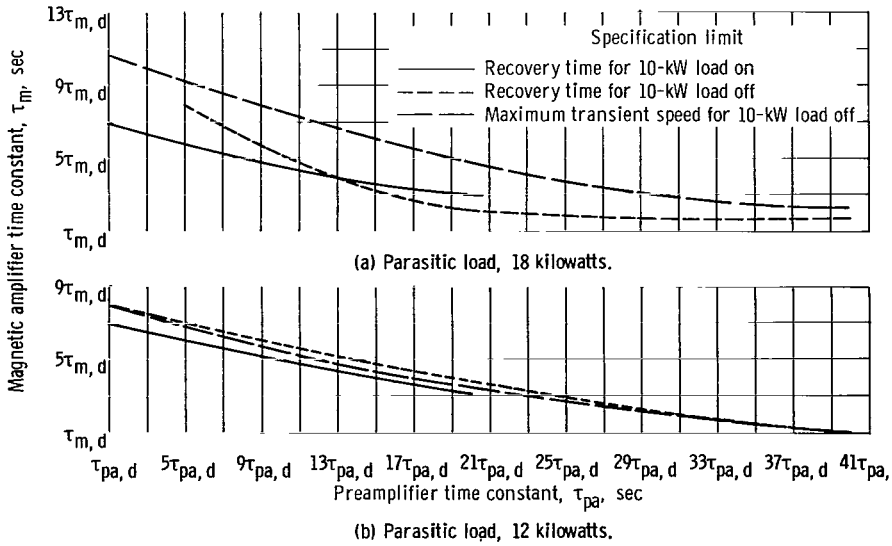

Figure 20. - Limits imposed on time constants by specifications. Magnetic amplifier design time constant $\tau_{m,d}$, 0.031 second; preamplifier design time constant $\tau_{pa,d}$, 0.005 second.

was the limiting factor for the 12-kilowatt parasitic-load control over the whole range but was the limiting factor over only part of the range for the 18-kilowatt capacity control. For the larger preamplifier time constants, the magnetic amplifier constant is limited by the recovery-time specification for the vehicle-load-off transient when the capacity of the parasitic load is 18 kilowatts. Therefore, the 18-kilowatt parasitic-load control has a somewhat smaller range of permissible variations in time constants than does the 12-kilowatt capacity control.

Stability

Stability of the speed control is an important factor to be considered in its design. With increasing time-constant combinations, the speed response to the removal of vehicle load becomes underdamped and oscillatory until certain values of preamplifier and magnetic amplifier time constants are reached, at which the speed oscillates with constant magnitude and frequency.

The speed-response damped frequency and amount of overshoot were plotted as functions of magnetic amplifier and preamplifier time constants for 10-kilowatt vehicle load stepped off with 18-kilowatt parasitic-load capacity in figure 21. The damped frequency

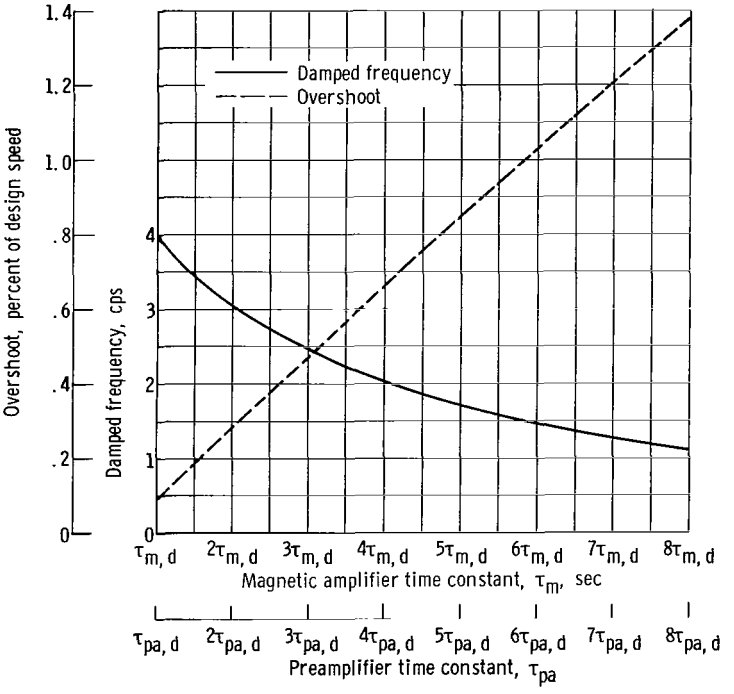

Figure 21. - Amount of overshoot and damped frequency as functions of control time constants. Magnetic amplifier design time constant $\tau_{m,d}$, 0.031 second; preamplifier design time constant $\tau_{pa,d}$, 0.005 second.

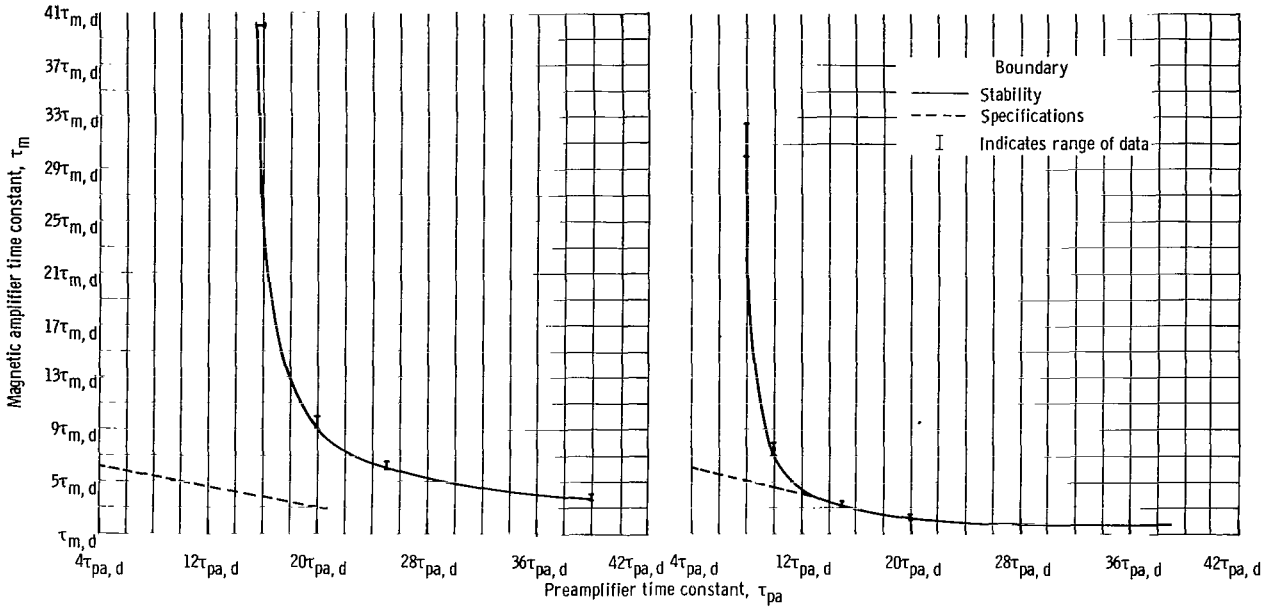

(a) Parasitic load, 12 kilowatts.

(b) Parasitic load, 18 kilowatts.

Figure 22. - Comparison of stability and specifications boundaries on time constants. Magnetic amplifier design time constant $\tau_{m,d}$, 0.031 second; preamplifier design time constant $\tau_{pa,d}$, 0.005 second.

ranges from 4 to 1 cps between design values and eight times design values of time constants. The percentage of overshoot increases from 0.1 to 1.4 percent over the same range of time constants. The percentage of overshoot in this figure is the difference between maximum transient and steady-state speed error, and the damped frequency is the frequency of the converging oscillation to the final steady-state point.

The stability boundary lines are compared with the limits imposed by the other specifications in figure 22 for 12- and 18-kilowatt parasitic loads. For the 12-kilowatt-capacity parasitic load (fig. 22(a)), all time-constant combinations for which speed response remains within specifications lie well within the stability boundary. For the 18-kilowatt-capacity load (fig. 22(b)), the stability margin is zero for some time constants which satisfy the specifications.

A speed response to stepwise removal of real load for one combination of time constants that results in instability is illustrated in figure 23. This instability occurs for $32.5\tau_m$ (1.007 sec) and $8\tau_{pa}$ (0.04 sec). The limit cycle is at 8 cps with a peak-to-peak amplitude of 0.9 percent of the 400-cps condition.

Stability of the speed controller with design time constants, but with increased controller gain, was also studied for an 18-kilowatt capacity parasitic load. In figure 24,

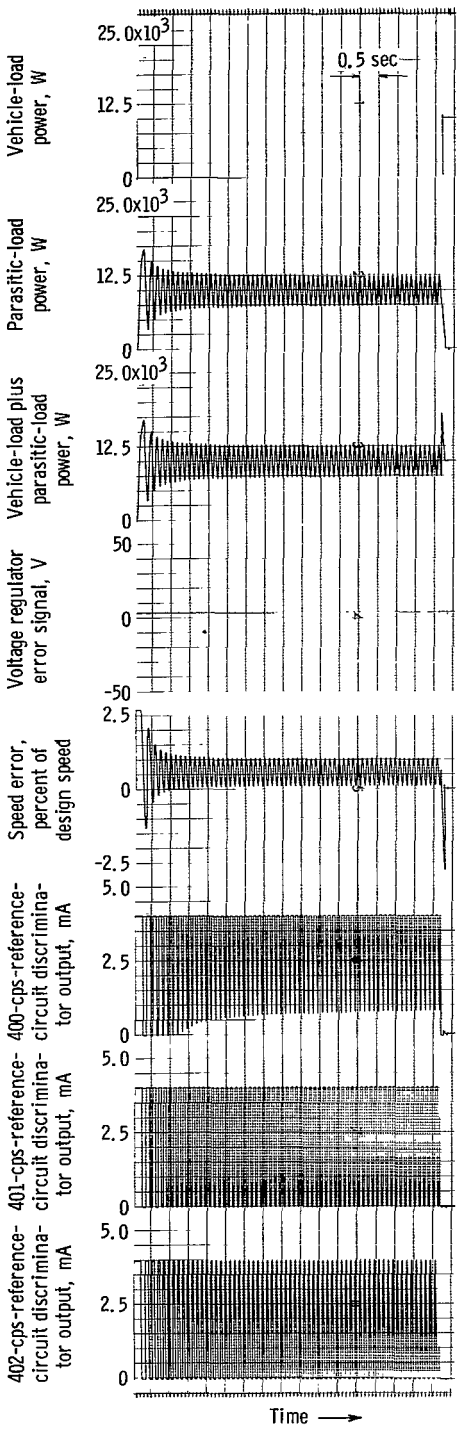

Figure 23. - Unstable response of system variables to stepwise removal of 10-kilowatt vehicle load. Parasitic load, 18 kilowatts; control time constants, 32.5 times magnetic amplifier design time constant and 8 times preamplifier design time constant.

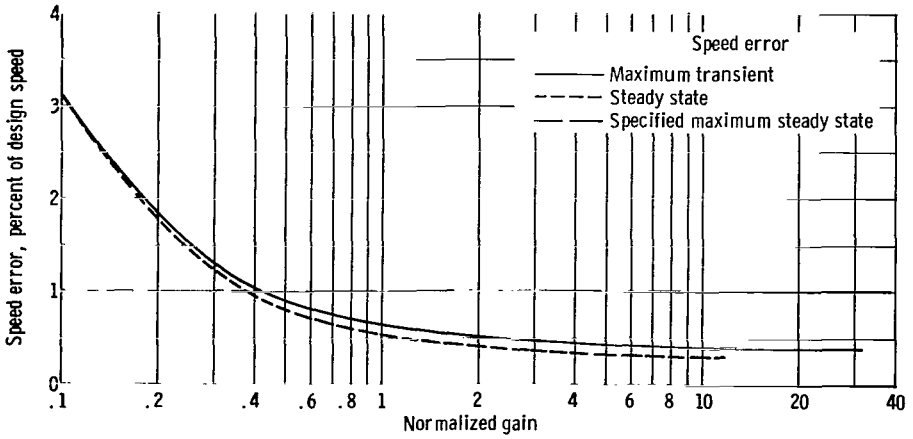

Figure 24. - Speed error as function of overall control gain. Parasitic load, 18 kilowatts; real load off transient, 10 kilowatts; design time constants.

normalized total gain is plotted as a function of speed error. A normalized gain of 1 corresponds to a total controller gain of 4000 watts per cps; this gain is the total gain for design parameters and an 18-kilowatt parasitic-load capacity (fig. 10(b), p. 12). As controller gain was increased, speed instability occurred when the gain was between 10 and 20 times design gain. The power dissipated in the parasitic load became oscillatory (with peak-to-peak amplitude between 5 and 10 kW), but the amplitude of the oscillation in speed was small (peak-to-peak amplitude about 0. 1 percent design speed) because of the attenuation factor of the turboalternator inertia. When the gain is decreased from design gain (normalized gain of 1) the curve indicates that the specifications will not be exceeded until the normalized gain is slightly less than 0. 4, at which point the steady-state errors exceed the 1-percent specification.

Interaction between the speed control, with design gain and time constants, and an unstable voltage regulator was investigated. The voltage regulator was made unstable by disconnecting the stabilizer circuit (i. e., setting the stabilizer gain equal to zero) (fig. 25). A sustained oscillation occurred in the line voltage (peak-to-peak amplitude, 43 V) and, therefore, in the alternator output power. Since the output power has a direct effect on speed, the speed became oscillatory, but the oscillations were attenuated by the speed control (peak-to-peak amplitude was less than 0. 2 percent at 7 cps). The speed control is aided, of course, by the large integrating effect of the turboalternator inertia.

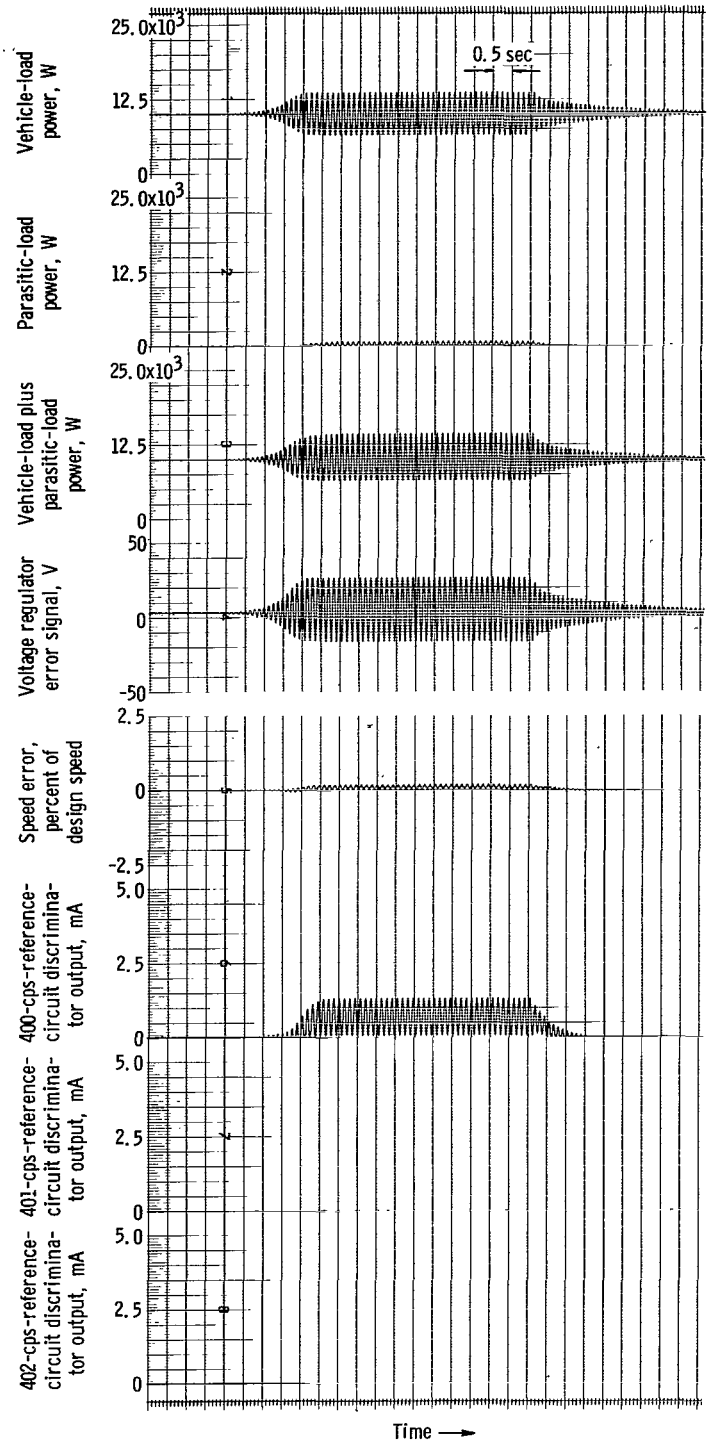

Figure 25. - Response of system variables to unstable voltage regulator. Parasitic load, 18 kilowatts; design control time constants.

CONCLUSIONS

An analog-computer study was made of a parasitic-load speed control for a 10-kilowatt solar-Brayton system turboalternator. For the particular transients studied and with design values of time constants and controller gain, the simulated speed control satisfied both the steady-state and the transient specifications with parasitic-load capacities equal to, or greater than, 10 kilowatts. A parasitic capacity greater than 10 kilowatts, however, is needed to ensure positive control with the vehicle load removed. In order to ensure positive control with full vehicle load applied, the speed control must maintain some parasitic power consumption at the design point of the power system.

The controller time constants can be several times larger than the design values for controllers with 12- and 18-kilowatt parasitic loads. The 18-kilowatt capacity controller has a slightly smaller permissible range of time constants than does the 12-kilowatt capacity controller. For a 12-kilowatt capacity load, instability occurs well beyond the range of time constants for which performance specifications are satisfied. The specification boundary and the stability boundary for an 18-kilowatt parasitic load appear to be coincident over part of the range investigated. When instability does occur, it is in the form of a sustained oscillation in speed.

Further investigation of controller instability revealed that, with design time constants, an increase in total gain by a factor of 10 can be tolerated before instability occurs, and further stability margin can be obtained since a decrease in total gain by a factor of 1/2 still allows performance within specifications with a parasitic load of 18 kilowatts.

Instability in the voltage regulator causes the speed control to oscillate with small sustained amplitude in speed.

Lewis Research Center,
National Aeronautics and Space Administration,
Cleveland, Ohio, September 23, 1966,
123-33-04-03-22.

APPENDIX - SYMBOLS

C_1	constant, 0.694 W/V^2
C_2	constant (0.232 for $P_{pℓt}$ = 10 kW, 0.278 for $P_{pℓt}$ = 12 kW, and 0.417 for $P_{pℓt}$ = 18 kW), W/V^2
e	frequency error, cps
f	frequency, cps
$f_{r,1}$	reference frequency, 400 cps
$f_{r,2}$	reference frequency, 401 cps
$f_{r,3}$	reference frequency, 402 cps
G	generator
$\mathscr{J}$	inertia of turboalternator, 0.051 (ft-lb)(sec^2)
I_d	discriminator output current, mA
I_f	field current, mA
I_m	magnetic amplifier output current, mA
$I_{m,0}$	magnetic amplifier output current for e = 0, 5 mA
I_{pa}	preamplifier output current, mA
$I_{pa,0}$	preamplifier output current for e = 0, 40 mA
$I_{pℓ}$	current into parasitic-load resistor, mA
K_c	controller gain
K_{cc}	comparison circuit
K_d	discriminator gain, 2mA/cps
K_g	generator gain
K_{gf}	generator field gain
K_m	gain of magnetic amplifier, -7.05
K_{pa}	gain of preamplifier, -9.5
$K_{pℓ}$	parasitic-load gain
K_{sc}	stabilizing circuit gain
K_{scw}	gain of saturable current potential transformer control winding
K_{se}	static exciter gain
K_{sr}	sensitizing rectifier gain
K_t	total controller gain
K_{tma}	transistor magnetic amplifier gain
K_{vd}	gain of voltage divider
K_α	gain of silicon controlled rectifier, 0.635^o/mA
N	speed of turboalternator, rps
ΔN	speed error, $N - N_r$, rps
N_r	reference speed, 200 rps
$P_{pℓ}$	total power into parasitic load, kW
$P_{pℓt}$	maximum power which can be dissipated by parasitic load, kW

$P_{pl,1}$	power into parasitic load controlled by 400-cps reference circuit, kW
$P_{pl,2}$	power into parasitic load controlled by 401-cps reference circuit, kW
$P_{pl,3}$	power into parasitic load controlled by 402-cps reference circuit, kW
P_t	turbine power, 10 kW
P_{tot}	total load power ($P_{vl} + P_{pl,1} + P_{pl,2} + P_{pl,3}$), kW
P_{vl}	power into vehicle load, kW
p	number of poles, four
T	torque
T_l	load torque, ft-lb
T_T	turbine torque, ft-lb
V_e	voltage regulator error
V_f	field voltage, V
V_{ln}	alternator line voltage, V
V_r	voltage reference, 12 V
α	silicon controlled rectifier firing angle, deg
τ_m	time constant of magnetic amplifier, sec
$\tau_{m,d}$	design time constant of magnetic amplifier, 0.031 sec
τ_{pa}	time constant of preamplifier, sec
$\tau_{pa,d}$	design time constant of preamplifier, 0.005 sec
$\varphi_A, \varphi_B, \varphi_C$	alternator phases

REFERENCES

1. Thomas, Ronald L.: Turboalternator Speed Control with Valves in Two-Spool Solar-Brayton System. NASA TN D-3783, 1966.

2. Hurrell, Herbert G.; and Thomas, Ronald L.: Control and Startup Considerations for Two-Spool Solar-Brayton Power System. NASA TM X-1270, 1966.

"The aeronautical and space activities of the United States shall be conducted so as to contribute . . . to the expansion of human knowledge of phenomena in the atmosphere and space. The Administration shall provide for the widest practicable and appropriate dissemination of information concerning its activities and the results thereof."

—NATIONAL AERONAUTICS AND SPACE ACT OF 1958

NASA SCIENTIFIC AND TECHNICAL PUBLICATIONS

TECHNICAL REPORTS: Scientific and technical information considered important, complete, and a lasting contribution to existing knowledge.

TECHNICAL NOTES: Information less broad in scope but nevertheless of importance as a contribution to existing knowledge.

TECHNICAL MEMORANDUMS: Information receiving limited distribution because of preliminary data, security classification, or other reasons.

CONTRACTOR REPORTS: Technical information generated in connection with a NASA contract or grant and released under NASA auspices.

TECHNICAL TRANSLATIONS: Information published in a foreign language considered to merit NASA distribution in English.

TECHNICAL REPRINTS: Information derived from NASA activities and initially published in the form of journal articles.

SPECIAL PUBLICATIONS: Information derived from or of value to NASA activities but not necessarily reporting the results of individual NASA-programmed scientific efforts. Publications include conference proceedings, monographs, data compilations, handbooks, sourcebooks, and special bibliographies.

Details on the availability of these publications may be obtained from:

SCIENTIFIC AND TECHNICAL INFORMATION DIVISION

NATIONAL AERONAUTICS AND SPACE ADMINISTRATION

Washington, D.C. 20546